Available online at www.sciencedirect.com
ScienceDirect
Nuclear Physics B Proceedings Supplement 00 (2014) 1–3
Nuclear Physics B Proceedings Supplement

Search for narrow scalar X → $\gamma\gamma$ in the mass range 65 − 600 GeV with the ATLAS detector

Zuzana Barnovska

LAPP, 9 Chemin de Bellevue, 74941, Annecy-le-Vieux, France

Abstract

A search for scalar narrow resonance X decaying into two photons in the mass range 65-600 GeV is performed using 20 fb^{-1} of pp collision data collected with the ATLAS detector at $\sqrt{s} = 8$ TeV at the Large Hadron Collider. The signal associated to the diphoton decay of the Higgs boson with a mass of 125.9 GeV is treated as a background. No significant evidence for an additional signal is observed. The result is presented as a model-independent limit on the production cross-section times the branching fraction BR (X → $\gamma\gamma$), in a fiducial volume where the reconstruction efficiency is independent of the event topology. The upper limits set extend over a considerably wider mass range than the limits previously set by the ATLAS and CMS collaborations.

Keywords: Higgs boson, diphoton resonance, ATLAS, LHC, pp collisions

The scalar boson of mass $m_{\mathrm{H}} \cong 126$ GeV, discovered at the LHC by ATLAS [1] and CMS [2], has properties compatible with those of the predicted Standard Model (SM) Higgs boson [3]. However, many models beyond the SM predict the existence of a second scalar particle with higher mass [4], while the NMSSM and 2HDM models [5] predict a new resonance with mass smaller than 126 GeV. The second resonance is expected to be narrow when its branching ratio to two photons is non-negligible. Therefore, the search for other Higgs-like states, presented here, focuses on a narrow resonance X in a wide mass range of $65 < m_{\mathrm{X}} < 600$ GeV.

The ATLAS experiment [6] at the Large Hadron Collider (LHC) is a multi-purpose experiment, covering a large range of pseudorapidity $|\eta| < 4.9$ and a full azimuth. It consists of an inner tracking detector covering the pseudorapidity range $|\eta| < 2.5$, surrounded by a thin superconducting solenoid, electromagnetic and hadronic calorimeters, large superconducting toroidal magnets and the muon spectrometer with end-caps.

This analysis was performed using 2012 proton-proton collision data at $\sqrt{s} = 8$ TeV, with a diphoton trigger requiring both photon candidates to have $E_{\mathrm{T}}^{\gamma} >$ 20 GeV and medium shower shape criteria. The data must fulfill the standard data quality requirements, with all ATLAS systems operational, corresponding to the total integrated luminosity of $\mathcal{L} = 20.3 \pm 0.6$ fb^{-1}. Photon candidates are selected in a region of $|\eta| < 2.37$, and tight cuts are applied on shower shape variables to reduce the background composed of QCD jets with leading neutral hadrons decaying into photons. The photon candidates are required to be isolated, where the p_{T} sum of all stable particles found within a cone of $\Delta R = \sqrt{\Delta\phi^2 + \Delta\eta^2} < 0.4$ around the candidate must be smaller than 6 GeV for $E_{\mathrm{T}}^{\gamma} \leq 80$ GeV and the same cut is applied on the quantity $I_{calo}^{corr} = I_{calo} - 0.7\%(E_{\mathrm{T}}^{\gamma} - 80$ GeV) for candidates with $E_{\mathrm{T}}^{\gamma} > 80$ GeV. In addition a cut on the track isolation $I_{track} = \sum p_{\mathrm{T}}^{PVtrack\,>1\ \mathrm{GeV}} < 2.6$ GeV within $\Delta R < 0.2$ excluding the conversion tracks and an offline cut of $E_{\mathrm{T}}^{\gamma} > 22$ GeV is applied.

The resonance with mass m_{X} is considered narrow when its intrinsic width is smaller than 0.09 GeV + $0.01 \times m_{\mathrm{X}}$. This upper limit is defined such that the bias in the number of fitted signal events is smaller than 10%. The width of the new resonance is then dominated by the experimental resolution in the ATLAS de-

tector. Model-dependent interference effects between the resonance and the continuum background are not considered. To increase the sensitivity, the search is split into two analyses: a categorized low-mass analysis ($65 < m_X < 110$ GeV) and an inclusive high-mass analysis ($110 < m_X < 600$ GeV). To provide sidebands for the fit of the $m_{\gamma\gamma}$ spectrum, the $m_{\gamma\gamma}$ ranges are wider than m_X ranges and overlap at the transition point.

The resonance X is modelled using POWHEG [7, 8] interfaced with PYTHIA8 [9] MC SM Higgs samples produced via gluon-gluon fusion (ggF), for masses of 70 – 1000 GeV, simulated with a width of 4 GeV. Consequently, the width of the simulated peak is dominated by the detector resolution (mostly its constant term, especially at high masses). Low and high mass tails are present, due to miscalibration (energy loss before the calorimeter) or material mismodelling. The Double-sided Crystal Ball function (DSCB), chosen to describe the shape, consists of a Gaussian core and a power law tail on the low and high mass sides and has six free parameters [10]. All MC samples are fitted individually, and the six fit parameters are parameterized w.r.t. m_X with an appropriate function (e.g. linear, quadratic). A categorized sample, containing several mass points, is then produced and simultaneously fitted. The shape of the parameters w.r.t. m_X is, in the case of the multiple mass point fit, restricted by the parameterizations obtained from the single mass point fits. The two fitting methods (single and multiple) produce results in very good agreement and the parameterization obtained from the multiple fit method is used. The signal modelling was done separately for the categorized low-mass analysis and the inclusive high-mass analysis.

The low-mass background includes the continuum diphoton background with dominantly $\gamma\gamma$, γ-jet and jet-jet events and Drell-Yan (DY) production (both resonant (Z) and non-resonant). To increase the sensitivity, the sample was split into three categories according to the number of conversions: two converted (CC), two unconverted (UU) and one converted, one unconverted (CU). The resonant background mostly comes from the CC category. In each category, the resonance shape is described by a DSCB function, parameters of which are determined by a fit to a dielectron data sample, where the electrons must satisfy the same requirements as the selected photon candidates. Most of the misidentified electrons underwent large bremsstrahlung, therefore, the $m_{ee'}$ distribution is wider and shifted to lower masses by up to 2 GeV compared to the Z boson reconstructed from true electron pairs. The $m_{ee'}$ distribution is therefore transformed by a shift in E_T and a smearing in ϕ. The obtained DY templates are normalized by

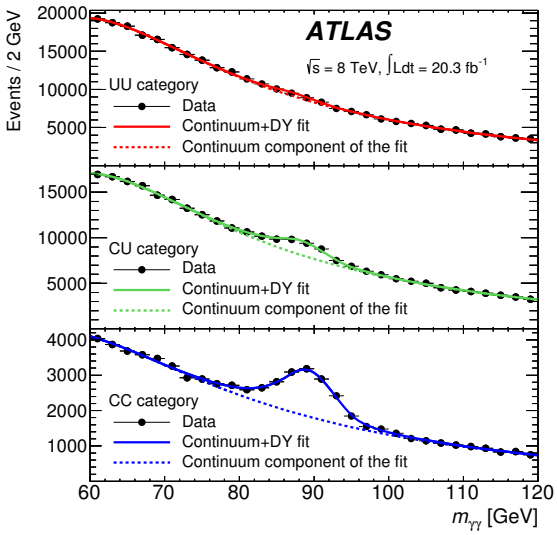

Figure 1: Background-only fits to the data (black dots) as functions of the diphoton invariant mass $m_{\gamma\gamma}$ for the three conversion categories in the low-mass range. The solid lines are fits of the sum of the DY and the Landau+exponential component. The dashed lines show the continuum component only.

factors computed from the $e \to \gamma$ fake rates, defined as the ratios of $e\gamma$ to ee pairs measured in $Z \to ee$ data. The function describing the diphoton continuum background is a sum of Landau and an exponential distribution over the full $m_{\gamma\gamma}$ low-mass range. The bias on the signal yield induced by the choice of the functional form is required to be lower than 20% of the statistical uncertainty on the fitted signal yield for the background-only spectrum. This was studied on an Asimov dataset [11]. Figure 1 shows background-only fits to the data in the low-mass region.

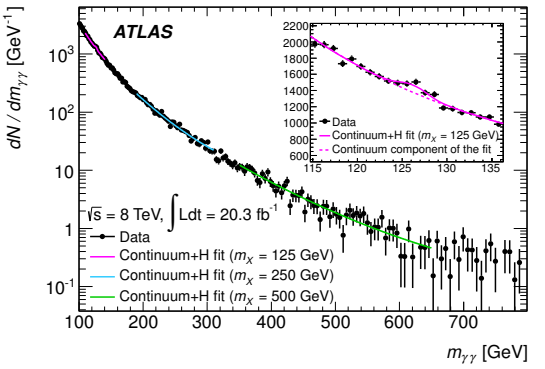

Figure 2: Background-only fits to the data (black dots) as functions of the diphoton invariant mass $m_{\gamma\gamma}$ for the inclusive high-mass analysis. The solid line shows the sum of the Higgs boson and the continuum background. The dashed line shows the continuum component only.

The high-mass analysis describes the continuum

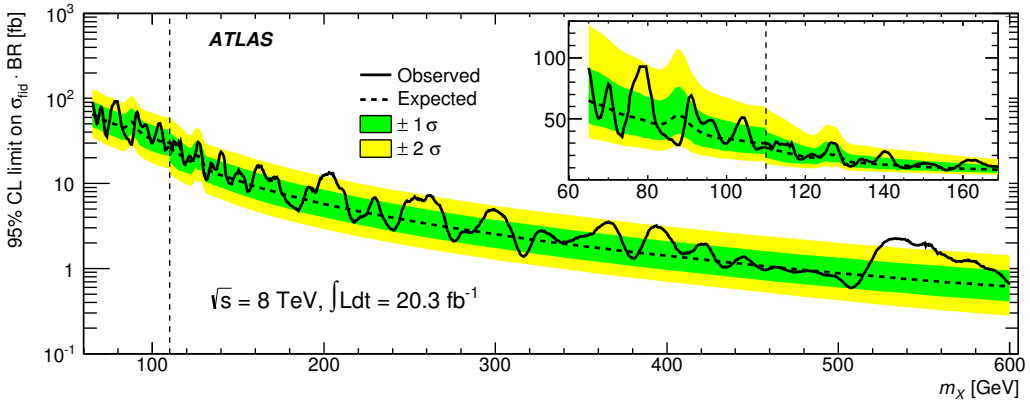

Figure 3: Observed and expected 95% C.L. limit on the $\sigma_{fid}.BR(X \to \gamma\gamma)$ as a function of m_X in the range $65 < M_X < 600$ GeV. The discontinuity in the limit at m_X (vertical dashed line) is due to the transition between the low-mass and the high-mass analyses. The green and yellow bands show the $\pm 1\sigma$ and $\pm 2\sigma$ uncertainties on the expected limit. The inset shows a zoom around the transition point.

background and the SM Higgs boson background. Relative cuts $E_T^{\gamma_1}/m_{\gamma\gamma} > 0.4$ and $E_T^{\gamma_2}/m_{\gamma\gamma} > 0.3$ are added to increase the signal sensitivity. The continuum background is fitted with an exponential of a second-order polynomial inside a sliding window of width $80.(m_X - 110\,\text{GeV})/110 + 20\,\text{GeV}$. The function and the fit window were determined by requiring the signal yield bias criteria introduced above. The background shape associated to the SM Higgs boson diphoton decays is modelled by a DSCB function normalized for $m_H = 125.9$ GeV [12, 13] using the most up to date theoretical inputs [16]. Figure 2 shows background-only fits to the data in the high-mass range.

The result of this analysis is presented in a fiducial volume defined by the E_T^γ cuts and the η region. In addition, the particle isolation should be $E_T^{iso} < 12$ GeV. The fiducial cross-section is computed using a C_X factor:

$$\sigma_{fid}.BR = \frac{N_{events}}{C_X.L}, \qquad C_X = \frac{N_{selection}}{N_{acceptance}} \qquad (1)$$

derived from the ggF samples, which ranges from 0.56 to 0.71 as a function of m_X, ensuring model independence of the result. The statistical analysis of the data uses unbinned maximum likelihood fits. The DY and Higgs shapes and normalizations are allowed to float within their uncertainties. Only two excesses with 2.1σ ($m_X = 201$ GeV) and 2.2σ ($m_X = 530$ GeV) local significances above the background are observed, which is consistent with the absence of a new narrow resonance in full the mass range of 65 – 600 GeV. A 95% limit on $\sigma_{fid}.BR(X \to \gamma\gamma)$ is computed as in [1] and shown in Figure 3. The systematic uncertainties are listed in Table 1. These results extend over a considerably larger range then previous searches done by ATLAS and CMS collaborations [17, 18], which only covered the range of 110 – 150 GeV.

Signal and Higgs boson yield		*Z component of Drell–Yan*	
Luminosity	2.8%	Normalization[2]	9–25%
Trigger	0.5%	Peak position[2]	1.5–3.5%
γ identification[1]	1.6–2.7%	Template shape[2]	1.5–3%
γ isolation[1]	1–6%	*Higgs boson background*	
Energy resolution[1 2]	10–40%	Cross-section[3]	9.6%
Signal and Higgs boson		Branching ratio	4.8%
Energy scale	0.6%	*C_X factor*	
Continuum $\gamma\gamma$, γ j, jj, DY		Topology[1]	3–15%
Signal bias[1]	1–67 ev.	Pile-up & U. E.[1]	1.4–3.2%

Table 1: Summary of the systematic uncertainties, [1] mass dependent, [2] category dependent, [3] factorization scale plus parton density function uncertainties [16].

References

[1] ATLAS Collaboration, Phys. Lett. B, 716,1-29, 2012.
[2] CMS Collaboration, Phys. Lett. B, 716, 30, 2012.
[3] ATLAS Collaboration, Phys. Lett. B 726, 88 (2013).
[4] LHC Higgs Cross Section Working Group, Handbook of LHC Higgs Cross Sections: 3.Higgs Properties, arXiv:1307.1347.
[5] T. Lee, Phys.Rev. D8 (1973) 1226-1239.
[6] ATLAS Collaboration, JINST 3 (2008) S08003.
[7] S. Alioli *et. al.*, J. High Energy Phys., 04(2009) 002.
[8] P. Nason and C. Oleari, J. High Energy Phys. 02 (2010) 037.
[9] T. Sjostrand *et. al.*, J. High Energy Phys. 05 (2006) 026.
[10] M. Oreglia, Ph.D. thesis, Stanford University [SLAC Report No. SLAC-R-0236, Appendix D, 1980].
[11] G. Cowan *et. al.*, Eur. Phys. J., C 71, 1554, (2011).
[12] J. Beringer *et. al.* (Particle Data Group), Phys. Rev. D 86, 010001 (2012) and 2013 partial update of the 2014 edition.
[13] Differences in m_H used here and in [14, 15] are covered by the energy scale uncertainties, listed in Table 1.
[14] ATLAS Collaboration, Phys. Rev. D 90, 052004 (2014).
[15] CMS Collaboration, Report No. CMS-PAS-HIG-14-009, 2014.
[16] S. Heinemeyer *et. al.*, LHC Higgs Cross Section Working Group, Report No. CERN-2013-004, 2013.
[17] ATLAS Collaboration, Phys. Lett. B 710, 538 (2012).
[18] CMS Collaboration, Phys. Rev. Lett. 108, 111801 (2012).